International Journal of GEOMATE, Oct., 2017, Vol.13, Issue 38, pp.149-156
Geotec., Const. Mat. & Env., ISSN:2186-2990, Japan, DOI: https://doi.org/10.21660/2017.38.61335

EFFECT OF LATERAL BOUNDARY CONDITION ON CONFINED - REINFORCED EARTH SUBJECTED TO DIFFERENTIAL SETTLEMENT

*Ho Manh Hung[1], Jiro Kuwano[1] and Shinya Tachibana[2]

[1]Department of Civil and Environmental Engineering, Saitama University, Japan
[2]Research Center for Urban Safety and Security, Kobe University, Japan

*Corresponding Author, Received: 10 April 2017, Revised: 1 May 2017, Accepted: 22 May 2017

ABSTRACT: A new method, the confined-reinforced earth (CRE) method, has been suggested to strengthen the subgrade layer, at the bottom of road pavement. The method uses granular soil, geogrids and confining tie rods. It is intended to reduce the damage from the large differential settlement between bridges or culverts and their approaches due to major earthquakes, and to make it possible for vehicles, especially emergency vehicles to pass the resulting unevenness. This study presents model tests designed to investigate the effects of the length of confined-reinforced earth by examining how lateral boundary conditions affect the consequences of differential settlement. Tests with two lateral boundary conditions, i.e. fixed-fixed (both ends of the geogrids are laterally fixed) and fixed-free (one end of the geogrid is laterally fixed and the other end is free) of the CRE method were performed and the effect of differential settlement was compared. The results show that the lateral boundary condition significantly affects the CRE behavior and the deformation in the fixed-fixed boundary condition is smaller than that in the fixed-free boundary condition.

Keywords: Confined-reinforced earth, Geogrid, Differential settlement and Lateral boundary condition

1. INTRODUCTION

Earthquakes often induce differential settlement between bridge abutments and approaches due to slope movement or grainslip [1]. In major seismic events, large deformations and significant differential settlement develop when liquefaction of the foundation occurs, resulting in cracking, settlement, lateral spreading and slumping [2]-[4]. Consequently, vehicles cannot pass the stepwise settlement created by the earthquake. Because of its high seismic resistance, geosynthetic reinforced soil has been widely used to mitigate such damage from earthquakes [5]-[7]. Furthermore, one important aspect of reinforced-soil is its potential to reduce differential settlement [8]-[11]. The confined-reinforced earth (CRE) method, has been proposed to make it possible for emergency vehicles to pass road surfaces roughened caused by earthquakes. The CRE method employs geogrid layers, prestressed steel tie rods, and granular soil applied to subgrade layers under paved roads. In this method, reinforced soil is confined by prestressed tie rods as shown in Fig. 1. A full-scale field test was previously carried out to compare the behavior of road structures, which were constructed by using the CRE method and a conventional method (without geosynthetics), when differential settlement of 550 mm was introduced into the supporting layer [12]. The results of trials with the two methods illustrated in Fig. 2 have shown that the road with CRE would allow a vehicle to pass while the other would not, because of a significant crack in the pavement. Reference [13] have also proved that the CRE method effectively improves the stiffness of the subgrade layer and can reduce a step-wise deformation of road pavement under differential settlement.

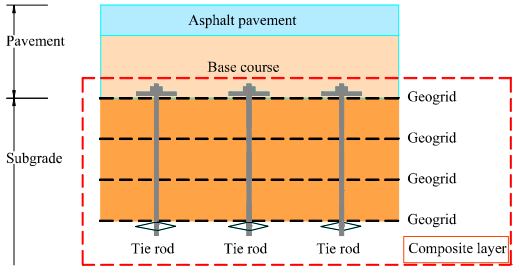

Fig. 1 Confined-reinforced subgrade (Adapted from [13])

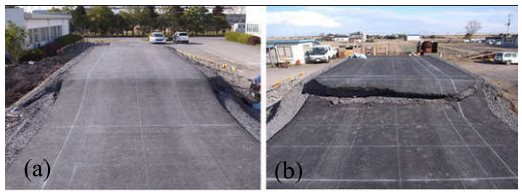

Fig. 2 Road deformation due to settlement, (a) with CRE method, (b) traditional method [12]

It has been noted that the key point of the CRE method, which makes it different from ordinary reinforced soil methods, is the confining tie rods. Prestress is introduced into the tie rods, contributing to the integrity of reinforced soil that

has high stiffness [14], [15]. As a result, deformation is reduced when it is subjected to differential settlement or traffic loading [16]. The prestress in tie rods strongly affects the CRE deformation.

In practice, CRE structures are not limited to a fixed length, though, previous experiments have not taken into account the effect of the length of the CRE on its behavior. For this issue, experiments with different lateral boundary conditions, i.e., both ends of the geogrids laterally fixed (fixed-fixed condition) and only one end of the geogrids laterally fixed (fixed-free condition) were performed. The fixed-fixed case simulates the condition in which one end of the geogrid is fixed on an abutment and the other end is embedded long enough so that the geogrid is not pulled out. The fixed-free case simulates a condition in which one end of a short geogrid is fixed on an abutment and the other end is embedded very short so that the geogrid is not fixed in the soil. Experiments with overburden stress, q, of 0 kPa and 4 kPa on the CRE surface simulating surcharge of the upper layers were carried out to investigate the deformation, strain in geogrid layers, reaction at both ends of the geogrids and force in the tie rods.

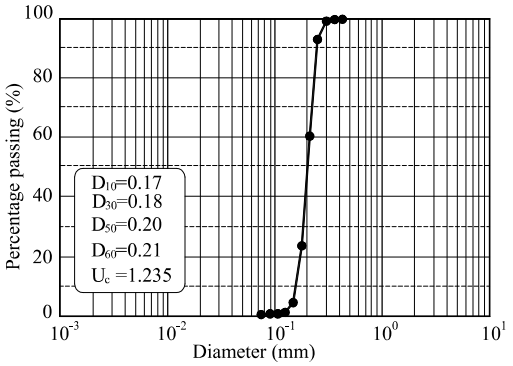

Fig. 3 Grain size distribution of Toyoura sand

2. TEST ON CONFINED-REINFORCED EARTH

2.1 Material properties

The geogrid (Adeam HG-200) used in this study is made of high density polyethylene with an opening size of 26 x 28 mm (longitudinal x transversal). The longitudinal rib is reinforced by aramid fibers. The geogrid has tensile strength of 200 x 5 kN/m (longitudinal x transversal) with rupture strain of 4.5 %. The granular soil used in the model was dry Toyoura sand (uniform sand) with specific gravity $\gamma_s = 2.645$; $e_{max} = 0.973$; $e_{min} = 0.609$; $D_{50} = 0.2$ mm. The internal friction angle of the dense sand is 42^0 at relative density of 80 % [17]. The grain size distribution is shown in Fig. 3.

2.2 Model test

The model test setup is shown in Fig. 4. The reinforced soil was made in a soil box with inner dimensions of length x width x height = 1200 mm x 400 mm x 800 mm. The composite layer was supported by two bottom plates, Plate 1 and Plate 2. Plate 1 was fixed on the frame (to simulate the abutment of a bridge or a culvert) while the other plate was supported by jacks so that it could move down to simulate settlement of the embankment below the pavement. Four geogrid layers (G1, G2, G3, G4) and three sand layers with the thickness of each layer of 100 mm were used. The lowest layer, G4, was placed directly onto the plates. Strain gauges were attached at four points, A, B, C, D as shown in Fig. 4a (at 300 mm, 500 mm, 700 mm, 900 mm from the left to right of the soil box, respectively) on each geogrid layer of G1, G2, G3, and G4. To measure both tensile strain and bending strain, pairs of strain gauges were attached on both sides of each point, i.e., on the upper and lower surfaces of the geogrid. Tie rods were set with spacing of 400 mm in the longitudinal direction and 200 mm in the transversal direction. They were placed at 200 mm, 600 mm and 1000 mm from the left to right of the soil box. It should be noted that in the fixed-fixed case, both ends of the geogrid were fixed in horizontal direction but free in vertical direction by using pulleys. While, in the fixed-free case, only one end of geogrid on Plate 1 is laterally fixed. (In order to prevent the sand from leaking when the CRE deformed, the sand layers were wrapped by thin low strength geotextile).

Table 1 Experimental cases

Cases	Lateral boundary conditions	Overburden, q (kPa)
Case 1	Fixed-fixed	0
Case 2	Fixed-free	0
Case 3	Fixed-fixed	4
Case 4	Fixed-free	4

2.3 Test procedures

Four experiments with different overburden stress (q) and lateral boundary condition were carried out. Test conditions are shown in Table 1. 4 kPa was applied as the overburden considering the field condition as shown in Fig. 2 (Ohta et al., 2013). The experimental procedure was as follows. In the first step, the lowest geogrid layer (G4) and six tie rods, R1 - R6 were placed on the bottom Plates 1 and 2. Then, the 100 mm - thick sand

layer was made by air pluviation technique as proposed by [18]. The sand was poured from a height of 45 cm using multiple sieve layers to achieve a constant relative density of approximately 80% (dense sand), and leveled. The other geogrid layers (G3, G2, G1) and upper sand layers were prepared in a similar way until completion. After the placement of the top geogrid (G1), the left end of the geogrids on the Plate 1 were all fixed in the horizontal direction by pulleys, whereas the right end of the geogrids on the Plate 2 were similarly fixed in the fixed-fixed cases or free in the fixed-free cases. The tie rods were then preloaded to 3 kN, a pressure high enough for effective CRE, but still well below failure level [15]. The allowable stress, q_a, on the soil (dense sand) is based on the ultimate bearing capacity of unreinforced soil, q_u, as proposed by [19] as cited by [20] for square footing as follows:

$$q_u = 1.3cN_c + qN_q + 0.4\gamma N_\gamma$$

where N_c, N_q and N_γ are the bearing capacity factors depending on the soil frictional angle, ϕ = 42°. q, c, γ are surcharge, cohesion and unit weight, respectively. Allowable stress is $q_a=q_u/FS$, in which FS is the safety factor, about 3 to 4. Therefore, $q_a=q_u/FS$= 1737/3.5=496 kN/m^2. The pressure on sand can be roughly calculated as force/area of the plate of the tie rod=3/(0.1*0.1)= 300 kN/m^2. In case of reinforced soil, the bearing capacity is larger compared to that of unreinforced soil [21]. Therefore, this pressure is low enough and acceptable. Then, overburden was applied. In the last step, Plate 2 supported by jacks was lowered to induce differential settlement, Sv, with respect to Plate 1. Lowering Plate 2 in Case 1 and 3 was stopped when the CRE layer was detached from the Plate 2. Responses of the CRE in Case 2 and Case 4 were compared with those at the same amount of settlement in Case 1 and Case 3 respectively. The deformation of the CRE surface was measured manually. The strains of the geogrid, reaction at the left side of the soil box and force in the tie rods monitored by strain gauges and load cells were recorded by the data recorder during the test.

3. RESULTS AND DISCUSSION

3.1 Surface settlement

Surface deformation due to the lowering of the bottom plate was measured at 100 mm intervals from the left to the right of the soil box. Figure 5 shows a typical tilting of the CRE due to settlement where clearly illustrates the displacement of the tie rods due to settlement, S_v (the rotation of tie rods was seen in all cases and the rotation of middle tie rods was larger compared with the other tie rods).

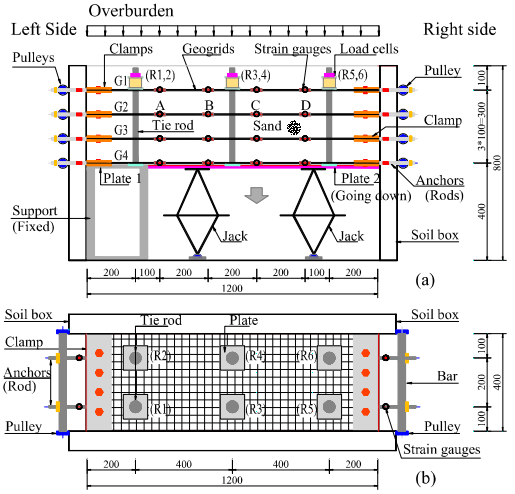

Fig. 4 Model test (Fixed-fixed case), (a) elevation view, (b) plan view

Distribution of the surface settlement in the four test cases were compared to investigate the effect of the lateral boundary conditions of the CRE on reducing the differential settlement at the surface. The distributions of the surface settlement are shown in Fig. 6 at Sv = 5 cm in Cases 1 and 2 and Sv = 9 cm in Case 3 and 4. It is to be noted that the surface settlement no more increased for the increase in Sv more than 5 cm in Case 1 (q = 0 kPa) and 9 cm in Case 3 (q = 4 kPa), when the geogrids were in fixed-fied conditions. On the other hand, in fixed-free conditions, the settlement increased more than 9 cm together with the increase in Sv. Therefore, in Fig. 6, distributions of the surface settlement are shown at Sv = 5 cm for Case 1 and 2 and at 9 cm for Case 3 and 4. Table 2 shows the slope of the surface in Case 1 and Case 2 for 5 cm settlement of Plate 2 and Case 3 and Case 4 for 9 cm settlement of Plate 2. The maximum slope surface was observed at 50 cm in all cases. As can be seen in Fig.6, at 5 cm settlement, the deformation in the first two cases without overburden stress, Case 1 and Case 2, was not much different (10 % of the maximum surface slope in Case 1 compared to 9.3% in Case 2 as shown in Table 2). This is because the settlement was small, resulting in small displacement of the CRE at the right side in Case 2. As a result, the boundary condition did not strongly affect the CRE deformation. However, in the cases with overburden stress of 4 kPa, Case 3 and Case 4, the deformation was clearly different (12.55% of the maximum surface slope in Case 3 compared to 21.35 % in Case 4 as illustrated in Table 2). This is due to the fact that in the fixed-fixed case, the right ends of the geogrids were restrained by boundary condition, resulting in reducing the CRE deformation while in the fixed-free case, the right ends were free, which allowed the right ends

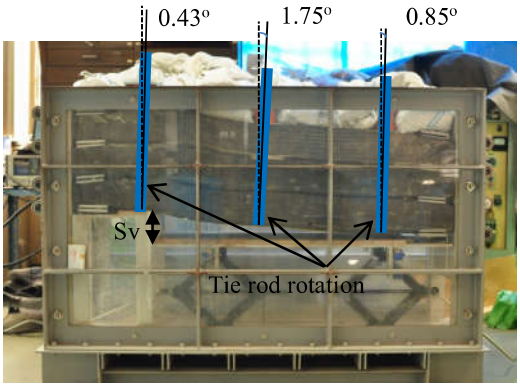

Fig. 5 Deformation of CRE in Case 3

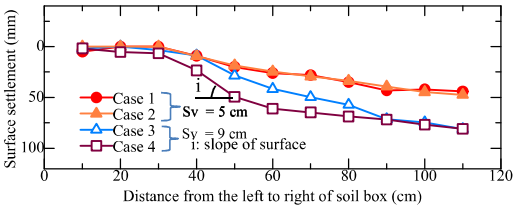

Fig. 6 Surface settlement due to the lowering of Plate 2

Table 2 Slope of surface at 30 cm, 50 cm and 70 cm

Cases	Slope of surface, i (%) at			Sv	q
	30 cm	50 cm	70 cm	cm	kPa
Case 1	2.50	10.0	4.00	5	0
Case 2	0.75	12.55	10.6	5	0
Case 3	0.00	9.30	5.35	9	4
Case 4	2.45	21.35	7.65	9	4

Sv: settlement of Plate 2
q: overburden

moved leftward. This explains why the deformation in Case 4 was larger than in Case 3.

3.2 Strains in the geogrid

Strain changes along the geogrids with the increase of S_v were monitored at four locations (A, B, C, D) as shown in Fig. 7 (Case 1), Fig. 8 (Case 2), Fig. 9 (Case 3) and Fig. 10 (Case 4). A positive strain value indicates the tensile deformation of the geogrid while a negative one means compression. In general, the tensile strain in the geogrid increased with an increase in settlement of Plate 2, S_v, in almost all the cases. However, strains of G4 was small and almost remained unchanged in Cases 2 and 4 of fixed-free condition. This is because the bottom layer in Case 2 and Case 4 could move leftward when the right end of the CRE was free, resulted in very small tensile or compressional deformation of G4. In the fixed-fixed cases (1 and 3), the highest strain was seen in

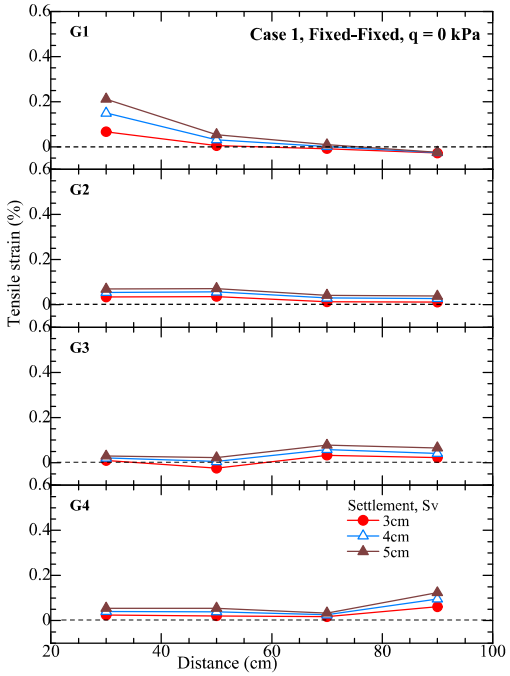

Fig. 7 Strain in geogrids of Case 1

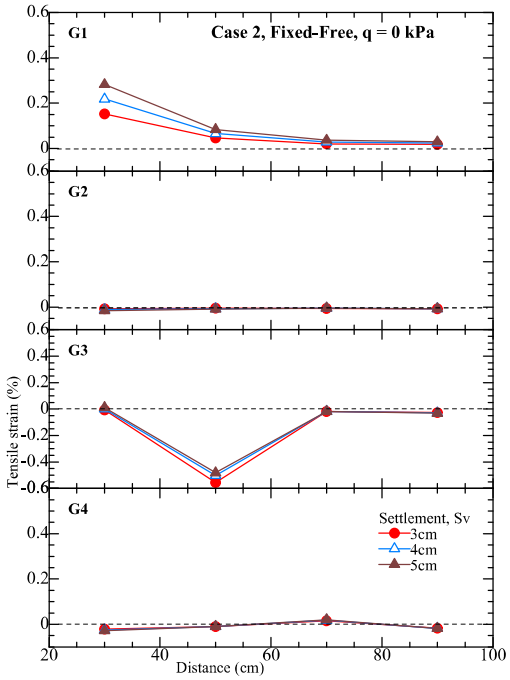

Fig. 8 Strain in geogrids of Case 2

G1 at A due to large rightward tilting of the middle tie rods, R3 and R4. The smallest strain was seen again in G1 but at D caused by clockwise rotation of the tie rods R5 and R6, though almost strains showed positive value, indicating tensile deformation of geogrids because tension must have developed in geogrids to support the vertical load by the membrane effect [22] like a hammock.

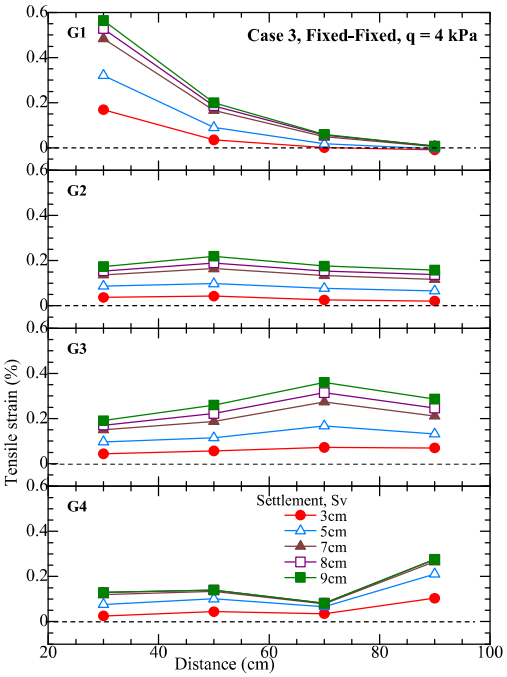

Fig. 9 Strain in geogrids of Case 3

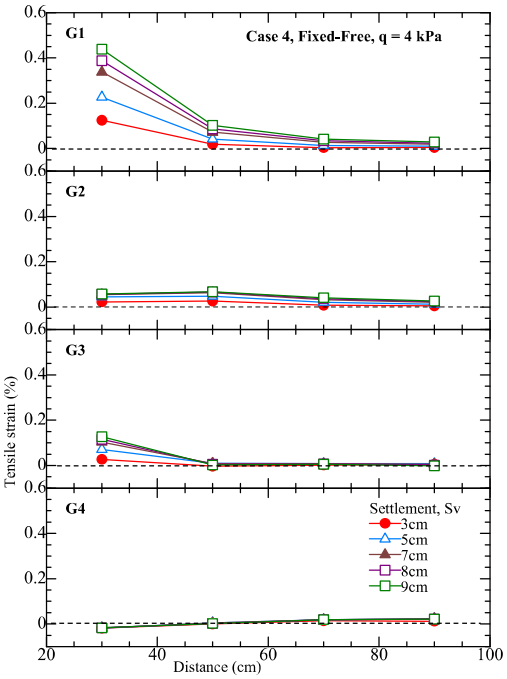

Fig. 10 Strain in geogrids of Case 4

It was also found in the fixed-fixed cases that the location of the peak strain shifted from point A in the top geogrid of G1 to point D in the bottom geogrid G4, i.e. the location of the highest strain shifted from the left to the right with depth. This is also because the mode of bending deformation of the CRE causing clockwise rotation of the tie rods as described above as seen in Fig. 5. By contrast, in the fixed-free cases, Case 2 and Case 4, the strain showed both tension and compression. This is because the mode of deformation in Case 2 and 4 was rather step-wise than a hammock and compressional deformation dominated at the bottom geogrid. The bottom of the tie rods R3 and R4 moved further left than in Case 1 and Case 3. Moreover, as can be seen from Fig.8, strain at B of G3 in Case 2 showed a large negative value (compression). It is due to the mode of CRE deformation was shown in Fig. 11. As schematically illustrated in Fig. 12, the CRE showed step-wise deformation, especially between R1, R2 and R3, R4. The upper layer of CRE was in tension, whereas the lower layer was in compression. In the case of G4, it was not in good contact with the soil layer as seen in Fig. 11 and could be free from compressional deformation of the lowest soil layer, so it was almost zero. On the other hand, in the case of G3, it was confined by the upper and lower soil layers and compressional deformation of the soil was reflected in the deformation of G3. This compressional strain was observed again in the repeated experiment with the same test condition.

The significant difference between the two series of cases, i.e. the fixed-fixed cases and the fixed-free cases, is that large tension developed in all geogrids in the fixed-fixed cases to support the vertical load whereas large tension was only observed at G1 in the fixed-free cases.

The tensile strain in all cases was maximum at point A in geogrid G1 (G1 A). Change in the tensile strain of G1 A is shown in Fig. 13 for an increase in settlement, Sv. It should be noted that the strain increased approximately linearly with the settlement.

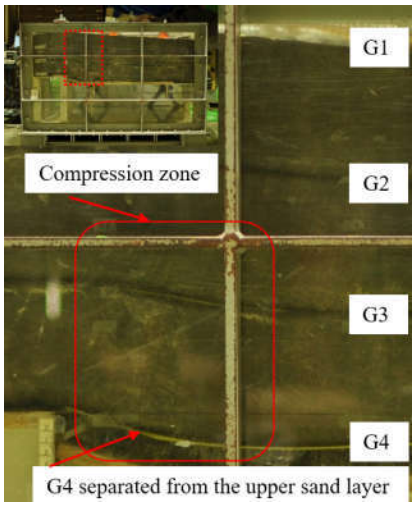

Fig. 11 CRE deformation (Case 2, Sv = 5 cm)

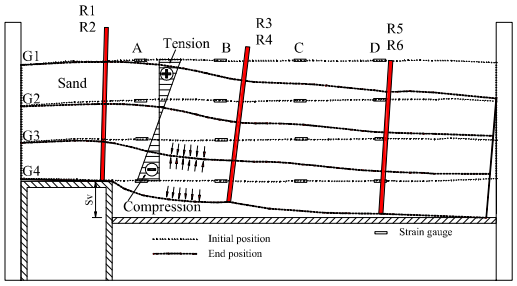

Fig. 12 Schematic view of CRE in Case 2 subjected to settlement

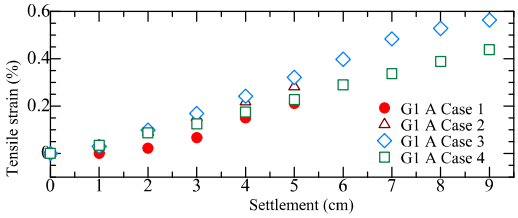

Fig. 13 Effect of settlement on strain in geogrids

3.3 Reaction at left end of the soil box

The reaction of geogrid layers, which were fixed to the soil box's left side by anchors, was measured and is shown in Figs. 14, 15, 16 and 17 (G1-4L are the reaction of the geogrids G1-4 at the left side, respectively). As with strain, a positive value indicates tension whereas a negative value indicates compression. In general, the total reaction of fixed-fixed cases was larger than that of fixed-free cases due to the restraint of right boundary condition, and the reaction in all four cases increased with overburden and settlement. In Case 1 and 2, the reaction was small and much smaller as compared to that in Case 3 and 4. The largest reaction in each case was observed at upper geogrids (G1, G2) while the lowest reaction occurred at G4; this is due to the rotation of the tie rods caused by the deformation of CRE layer, i.e. the top of tie rods R1 and R2 moved rightward while the bottom of the tie rods R3 and R4 moved leftward (Fig. 5).

3.4 Force in tie rods

Forces in the six tie rods, R1, R2, R3, R4, R5 and R6 were measured by the load cells while settlement of Plate 2 increased (Fig. 18). The tie rods were preloaded to 3 kN. However, the preload then decreased gradually before the increase of settlement because of stress relaxation of the soil. The rate of relaxation can be decreased significantly by applying sufficiently large preload during construction and allowing sufficiently large creep deformation of the soil to occur during

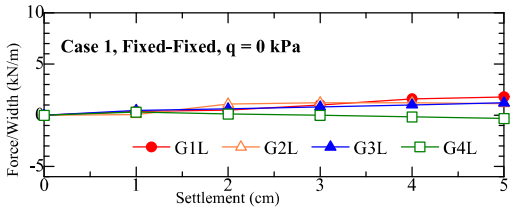

Fig. 14 Reaction at left side in Case 1

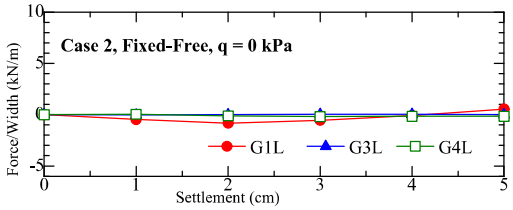

Fig. 15 Reaction at left side in Case 2

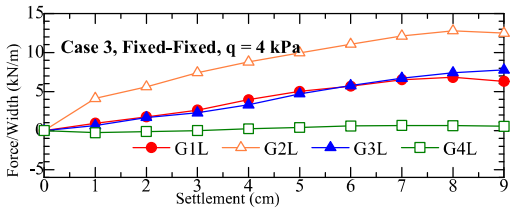

Fig. 16 Reaction at left side in Case 3

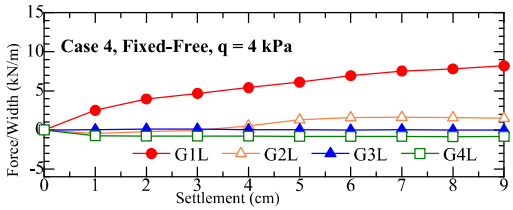

Fig. 17 Reaction at left side in Case 4

preloading [14]. As can be seen from Fig. 5, shear deformation in the CRE was predominant near the tie rods R3 and R4. When dense sand is sheared, it initially shows volume decrease within the small strain range. However, the dense sand then shows volume increase with increase in shear strain. Decrease in force in tie rods of four cases was observed in general. However, the tension in R3 and R4 recovered after the slight decrease probably due to dilatancy of the dense sand confined between geogrids in tension after certain amount of shear strain in the fixed-fixed case (Case 3). To the contrary, in Case 4 of fixed-free condition, tension in the geogrids was much less as compared to in Case 3 of fixed-fixed condition and the confinement of sand was much less. The sand particles could move more freely in Case 4 than in Case 3 as schematically illustrated in Fig. 19. It resulted in no recovery of the tension in the R3 and R4 in Case 4 even after a certain amount of shear deformation of the dense sand.

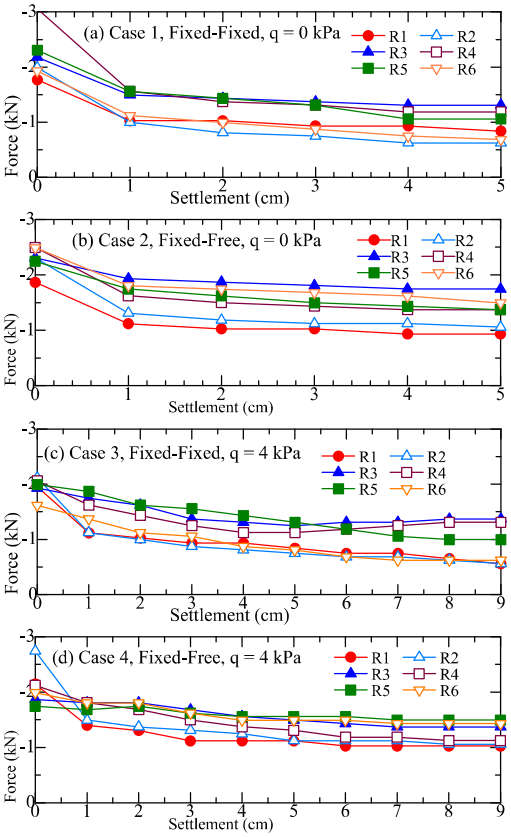

Fig. 18 Force in tie rods due to settlement

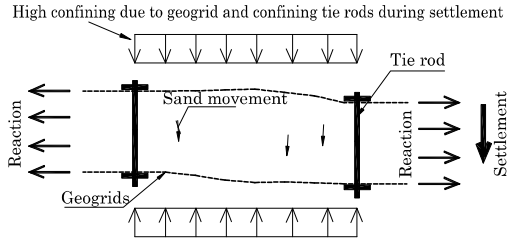

(a) Fixed-Fixed condition

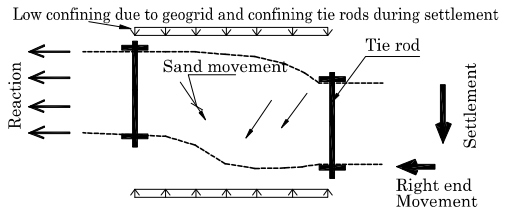

(b) Fixed-Free condition

Fig. 19 Sand particles movement due to settlement

4. CONCLUSIONS

A series of laboratory model tests was carried out to investigate the effect of lateral boundary conditions on the behavior of confined-reinforced earth (CRE). The following conclusions were obtained:

1) The lateral boundary condition strongly affects the behavior of CRE. The deformation of the CRE in the fixed-fixed case is smaller than that in the fixed-free case.

2) In the fixed-fixed case, all geogrid layers work simultaneously to support the vertical load, whereas in the fixed-free case, most of the vertical load is supported by the top layer, which is seen large tension, at a given amount of settlement.

3) The tensile strain in the geogrid increases almost linear with the increase in differential settlement between the two bottom plates. The location of high strain in fixed-fixed condition shifted from the left to the right with depth due to the rotational stepwise deformation of CRE with differential settlement between two bottom plates.

4) An increase in the confining stress of soil with shear deformation of CRE can be expected due to dilatant behavior of dense sand if the soil is well compacted and confined with geogrids and tie rods. An increase in the confining stress increases in the stiffness of the soil and therefore decreases the deformation of CRE.

REFERENCES

[1] Siddharthan, R. and El-Gamal, M (1996). "Earthquake-induced ground settlements of bridge abutment fills", Proceeding of ASCE National Convention, Washington, DC, pp, 100-123.

[2] Tani, S. (1996). "Damage to earth dams". Soils and Foundations. Spec. Issue on Geotech. Aspects of the January 17, 1995 Hyogoken-Nambu Earthquake. Japanese Geotech.Soc., Tokyo, Japan, 263-272.

[3] Abdel-Haq, A. and Hryciw, R. (1998). "Ground Settlement in Simi Valley following the Northridge Earthquake", J. Geotech. Geoenviron. Eng., 10.1061/(ASCE)1090-0241(1998)124:1(80), 80-89.

[4] Manika, M and Takahashi, A (2014) "Liquefaction-induced deformation of earthen embankments on non-homogeneous soil deposits under sequential ground motions", Soil Dynamics and Earthquake Engineering 66 (2014) 113-124.

[5] Tatsuoka, F., Tateyama, M., Uchimura, T. and Koseki, J., "Geosynthetic-reinforced soil retaining walls as important permanent Structures", Geosynthetics international, Vol.4, No.2, pp.81-136, 1997a.

[6] Koseki, J., "Use of geosynthetics to improve seismic performance of earth structures", Geotextiles and Geomembranes 34, pp.51-68, 2012.

[7] Kuwano, J., Miyata, Y. & Koseki, J. "Performance of reinforced soil walls during the 2011 Tohoku earthquake". Geosynthetics International, 21, No. 3, 179–196, 2014.
[8] Monley, G. and Wu, J.T.H. (1993). "Tensile Reinforcement Effects on Bridge-Approach Settlement", Journal of Geotechnical Engineering, ASCE, Vol. 119, No. 4, pp. 749-762.
[9] Helwany, S., Wu, J.T.H., and Froessl, B. (2003). "GRS Bridge Abutments – An Effective Means to Alleviate Bridge Approach Settlement", Geotextiles and Geomembranes, 21, pp. 177-196.
[10] Miao,L., Wang, F., Han, J. and Lv, W. (2004). "Benefits of geosynthetic reinforcement in widening of embankments subjected to foundation differential settlement", Geosynthetics International, 21, pp. 321-332.
[11] Viswanadham B.V.S. and Konig, D. (2009) "Centrifuge modeling of geotextile-reinforced slopes subjected to differential settlements", Geotextiles and Geomembranes, 27, pp.77-88.
[12] Ohta, H., Ishigaki, T., Tatta, N., "Retrofit technique for asphalt concrete pavements after seismic damage", Proceedings of the 18th International Conference on Soil Mechanics and Geotechnical Engineering, Paris, pp.1333-1336, 2013.
[13] Kuwano, J., Tachibana, S., Ishigaki, T. and Tatta, N. "Confined-reinforced subgrade to reduce differential settlement of road pavement". Proceedings of 5th KGS-JGS Geotechnical Engineering Workshop, Seoul, Korea, pp.149-154, 2013.
[14] Tatsuoka, F., Uchimura, T. and Tateyama, M., "Preloaded and prestressed reinforced soil", Soils and Foundations, Vol.37, No.3, pp.79-94, 1997b.
[15] Uchimura, T., Tateyama, M., Koga, T., Tatsuoka, F., "Performance of a preloaded and prestressed geogrid-reinforced soil pier for a railway bridge", Soils and Foundations, Vol.43, No.6, pp. 33-50, 2003.
[16] Shinoda, M., Uchimura, T. and Tatsuoka, F., "Increasing the stiffness of mechanically reinforced backfill by preloading and prestressing", Soils and Foundations, Vol.43, No.1, pp.75-92, 2003.
[17] Fukushima, S., and Tatsuoka, F.: strength and deformation characteristics of saturated sand at extremely low pressure, Soils and Foundations, Vol.24, No.4, pp. 30-48, 1984.
[18] Miura, S. and Toki, S. (1982)." Sample preparation method and its effect on static and cyclic deformation — strength properties of sand", Soils and Foundations, 22, pp. 61-77.
[19] Terzaghi, K. (1943). "Theoretical Soil Mechanics", John Wiley, New York.
[20] Das, B M. (1999). "Shallow foundation: bearing capacity and settlement", CRC Press, Florida, USA.
[21] Patra, C.R., Das, B.M., Atalar, C.: Bearing capacity of embedded strip foundation on geogrid-reinforced sand, Geotextiles and Geomembranes, 23, pp. 454-462, 2005.
[22] Holtz, RD., Christopher, BR., Berg, RR., "Geosynthetic design and construction guidelines", U.S. Department of Transportation Washington, D.C., 1998.